Pergamon

Int. J. Solids Structures Vol. 34, No. 7, pp. 837–846, 1997

0020-7683/97 $17.00 + .00

PII: S0020-7683(96)00056-X

A GENERALIZED APPROACH FOR IMPLEMENTING GENERAL BOUNDARY CONDITIONS IN THE GDQ FREE VIBRATION ANALYSIS OF PLATES

C. SHU
Department of Mechanical and Production Engineering, National University of Singapore, 10 Kent Ridge Crescent, Singapore 0511

and

H. DU
School of Mechanical and Production Engineering, Nanyang Technological University, Nanyang Avenue, Singapore 2263

(*Received* 12 *April* 1995; *in revised form* 10 *April* 1996)

Abstract—A new approach for implementing general boundary conditions in the GDQ free vibration analysis of rectangular plates is presented in this paper. The proposed approach directly couples the boundary conditions with the governing equations and is referred to as the CBCGE approach. It can be applied to any combination of simply supported, clamped, and free boundary conditions. The generality and accuracy of the CBCGE approach are demonstrated through its application to the vibration analysis of a rectangular plate with various combinations of free edges and corners. In particular, the effect of grid point distribution on the numerical results for plates with free boundary conditions is discussed, and a new grid point distribution is suggested. © 1997 Elsevier Science Ltd. All rights reserved.

1. INTRODUCTION

In the earlier companion paper of Shu and Du (1997), we proposed an approach for implementing the simply supported and clamped boundary conditions in the GDQ free vibration analysis of beams and rectangular plates. This approach substitutes all the boundary conditions into the governing equations and is referred to as the SBCGE method. In SBCGE, all the boundary conditions are discretized exactly at the boundary points. The SBCGE approach overcomes the drawbacks of the so-called δ-technique (see, e.g., Jan *et al.* (1989), Bert *et al.* (1993)), where the derivative boundary conditions are approximately discretized at a δ-point which is a distance δ away from the boundary. The numerical results obtained by the δ-technique may depend on the choice of the value of δ. To obtain accurate numerical results, δ should be chosen to be very small to minimize the effect of inappropriate implementation of derivative conditions at the δ-points. This can be done in a trial and test manner. In contrast, the SBCGE method introduced in Shu and Du (1997) does not need such a process since the derivative conditions are exactly discretized at the boundary points. Some comparisons between the SBCGE approach and the method of modifying weighting coefficient matrices (WMCM) (see, e.g., Wang and Bert (1993)) were also made in Shu and Du (1997) through their applications to the free vibration analysis of beams and rectangular plates. It was found that the SBCGE method works uniformly well for any combination of simply supported and clamped boundary conditions. The SBCGE method overcomes the drawback of the MWCM method for the case where the opposite edges or ends are clamped. For the details of SBCGE, see Shu and Du (1997).

As mentioned earlier, the basic idea of the SBCGE approach is to substitute all the boundary conditions into the discretized governing equations. This can only be done when the boundary conditions are simple. For example, as illustrated in Shu and Du (1997), when the clamped and simply supported boundary conditions are considered, the discretized derivative conditions only involve the function values along one mesh line. Thus, the

derivative conditions at two opposite edges or ends can be coupled to provide two solutions at two adjacent points of boundaries. These solutions can then be substituted into the governing equations. However, as can be seen in the following, for the free edge of a plate, the discretized boundary conditions involve all the function values in the whole computational domain. Thus, it is difficult to obtain explicit formulations for solutions at adjacent points of boundaries. In other words, the SBCGE method cannot be applied to such cases. This difficulty can be removed by a method proposed in this paper, which directly couples the discretized boundary conditions with the discretized governing equations. For simplicity, this method is called the CBCGE method. In this paper, the proposed CBCGE method will be applied to a variety of plate configurations with at least one free edge. Particularly, the effect of grid point distribution on the numerical results is discussed, and a new grid point distribution is suggested to obtain more accurate numerical results for plates with free edge and corner conditions.

2. GOVERNING EQUATIONS

The non-dimensional governing equation for a thin rectangular plate may be written as

$$\frac{\partial^4 W}{\partial X^4} + 2\lambda^2 \frac{\partial^4 W}{\partial X^2 \partial Y^2} + \lambda^4 \frac{\partial^4 W}{\partial Y^4} = \Omega^2 \cdot W \tag{1}$$

where W is the dimensionless mode shape function; Ω is the dimensionless frequency; $X = x/a$, $Y = y/b$ are dimensionless coordinates; a and b are the lengths of the plate edges; and $\lambda = a/b$ is the aspect ratio. Further, $\Omega = \omega a^2 \sqrt{\rho/D}$, where ω is the dimensional circular frequency, $D = Eh^3[12(1-\nu^2)]$ is the flexural rigidity, E, ν, ρ and h are Young's modulus, Poisson's ratio, the density of the plate material, and the plate thickness, respectively. Equation (1) is a 4th order partial differential equation with respect to X and Y. It requires two boundary conditions at each edge. In the present paper, the following three types of boundary conditions are considered.

Simply supported edge (SS)

$$W = 0, \frac{\partial^2 W}{\partial X^2} = 0 \tag{2a}$$

at X = constant, and

$$W = 0, \frac{\partial^2 W}{\partial Y^2} = 0 \tag{2b}$$

at Y = constant.

Clamped edge (C)

$$W = 0, \frac{\partial W}{\partial X} = 0 \tag{3a}$$

at X = constant, and

$$W = 0, \frac{\partial W}{\partial Y} = 0 \tag{3b}$$

at Y = constant.

Free edge (F)

$$\frac{\partial^2 W}{\partial X^2}+\nu\cdot\lambda^2\cdot\frac{\partial^2 W}{\partial Y^2}=0,\frac{\partial^3 W}{\partial X^3}+(2-\nu)\cdot\lambda^2\cdot\frac{\partial^3 W}{\partial X\partial Y^2}=0 \tag{4a}$$

at X = constant, and

$$\lambda^2\cdot\frac{\partial^2 W}{\partial Y^2}+\nu\cdot\frac{\partial^2 W}{\partial X^2}=0,\lambda^2\cdot\frac{\partial^3 W}{\partial Y^3}+(2-\nu)\cdot\frac{\partial^3 W}{\partial X^2\partial Y}=0 \tag{4b}$$

at Y = constant, and

$$\frac{\partial^2 W}{\partial X\partial Y}=0 \tag{4c}$$

at the corner of two adjacent free edges.

3. IMPLEMENTATION OF GENERAL BOUNDARY CONDITIONS

In the present work, the GDQ method is used to discretize the derivatives involved in the governing differential equation and the boundary conditions. The details of the GDQ method are shown in Shu and Du (1997). Supposing that there are N grid points in the X direction and M grid points in the Y direction, then the total number of function values in the whole computational domain is $N\times M$. Using the GDQ method, eqn (1) can be discretized as

$$\sum_{k=1}^{N} c_{i,k}^{(4)}\cdot W_{k,j}+2\lambda^2\cdot\sum_{k1=1}^{N}\sum_{k2=1}^{M} c_{i,k1}^{(2)}\cdot c_{j,k2}^{(2)}\cdot W_{k1,k2}+\lambda^4\cdot\sum_{k=1}^{M} c_{j,k}^{(4)}\cdot W_{i,k}=\Omega^2\cdot W_{i,j} \tag{5}$$

where $c_{i,k}^{(n)}$, $c_{j,k}^{(m)}$ are the GDQ weighting coefficients related to the derivatives $\partial^n W/\partial X^n$, $\partial^m W/\partial Y^m$, respectively. As demonstrated in Shu and Du (1997), the two boundary conditions at each edge of a rectangular plate provide two equations at each boundary point. Therefore, discretization of the boundary conditions at all boundary points would give $(4N+4M-16)$ equations. As we know, for a well-posed problem, the number of unknowns should be equal to the number of equations. Since the total number of unknowns is $N\times M$, the discretized governing eqn (5) should only be applied at $(N\times M-4N-4M+16)$ interior grid points. As shown in Fig. 1, this can be done by applying eqn (5) at interior grid points X_i, Y_j with $3\leqslant i\leqslant N-2$ and $3\leqslant j\leqslant M-2$. The derivatives involved in the boundary conditions can also be discretized by the GDQ method. For illustration, a plate configuration of C-SS-F-F is chosen to demonstrate the implementation of the boundary conditions. After GDQ discretization, the discretized boundary conditions along the four edges of the rectangular plate can be written as

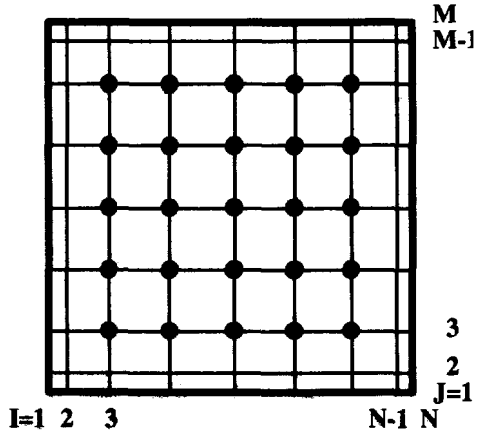

Fig. 1. Illustration of interior points for a rectangular plate.

$$W_{1,j} = 0 \tag{6a}$$

$$\sum_{k=1}^{N} c_{1,k}^{(1)} \cdot W_{k,j} = 0 \tag{6b}$$

for the edge of $X = 0$

$$\sum_{k=1}^{N} c_{N,k}^{(2)} \cdot W_{k,j} + v \cdot \lambda^2 \cdot \sum_{k=1}^{M} \bar{c}_{j,k}^{(2)} \cdot W_{N,k} = 0 \tag{7a}$$

$$\sum_{k=1}^{N} c_{N,k}^{(3)} \cdot W_{k,j} + (2-v) \cdot \lambda^2 \cdot \sum_{k1=1}^{N} \sum_{k2=1}^{M} c_{N,k1}^{(1)} \cdot \bar{c}_{j,k2}^{(2)} \cdot W_{k1,k2} = 0 \tag{7b}$$

for the edge of $X = 1$

$$W_{i,1} = 0 \tag{8a}$$

$$\sum_{k=1}^{M} \bar{c}_{1,k}^{(2)} \cdot W_{i,k} = 0 \tag{8b}$$

for the edge of $Y = 0$

$$\lambda^2 \sum_{k=1}^{M} \bar{c}_{M,k}^{(2)} \cdot W_{i,k} + v \cdot \sum_{k=1}^{N} c_{i,k}^{(2)} \cdot W_{k,M} = 0 \tag{9a}$$

$$\lambda^2 \sum_{k=1}^{M} \bar{c}_{M,k}^{(3)} \cdot W_{i,k} + (2-v) \cdot \lambda^2 \cdot \sum_{k1=1}^{N} \sum_{k2=1}^{M} c_{i,k1}^{(2)} \cdot \bar{c}_{M,k2}^{(1)} \cdot W_{k1,k2} = 0 \tag{9b}$$

for the edge of $Y = 1$

It is noted that eqns (7) and (9) involve all the function values in the whole computational domain. Thus, it is very difficult to couple eqns (6) and (7) or eqns (8) and (9) together to obtain analytical expressions for the solution of $W_{2,j}$, $W_{N-1,j}$, or $W_{i,2}$, $W_{i,M-1}$, as done in the SBCGE approach. However, as shown above, there are two boundary equations at each boundary point. One equation can be counted as the equation for the boundary point itself, and the other is counted as the equation for its adjacent interior point. In other words, eqns (6a), (7a), (8a), (9a) are counted as the equations for the boundary points themselves, while eqns (6b), (7b), (8b), (9b) are counted as the equations for their adjacent interior points. For example, eqn (6b) is taken as the equation for the adjacent interior points $i = 2, j = 2, 3, \ldots, M-1$. At four corners, the discretized boundary conditions can be written as

$$W_{1,1} = 0, \quad W_{N,1} = 0, \quad W_{1,M} = 0 \tag{10a}$$

$$\sum_{k1=1}^{N} \sum_{k2=1}^{M} c_{N,k1}^{(1)} \cdot \bar{c}_{M,k2}^{(1)} \cdot W_{k1,k2} = 0. \tag{10b}$$

Equation (10b) involves all the function values in the whole computational domain which cannot be substituted into the governing eqn (5) as is done in the SBCGE approach. This difficulty can be removed by the proposed method of coupling boundary conditions directly with the governing equations (CBCGE). In the CBCGE method, the function values in the whole domain are decomposed into two portions. One is based on the interior points where the governing equations are applied as shown in Fig. 1. The function values of this portion can be represented by a vector $\{W_I\}$. The remaining function values are based on the boundary points and their adjacent interior points, which can be denoted by a vector $\{W_B\}$. The ij component of $\{W_I\}$ can be defined by

$$\{W_I\}_{ij} = W_{i,j} \tag{11}$$

where

$$ij = (M-4)\cdot(i-3)+j-3+1, 3 \leqslant i \leqslant N-2, 3 \leqslant j \leqslant M-2.$$

The ij component of $\{W_B\}$ is defined by

$$\{W_B\}_{ij} = W_{i,j} \tag{12}$$

where

$$ij = \begin{cases} (i-1)\cdot M+j & \text{when } 1 \leqslant i \leqslant 2, 1 \leqslant j \leqslant M \\ 2M+4\cdot(i-3)+j & \text{when } 3 \leqslant i \leqslant N-2, 1 \leqslant j \leqslant 2 \\ 2M+4\cdot(i-3)+2+j-M+2 & \text{when } 3 \leqslant i \leqslant N-2, M-1 \leqslant j \leqslant M \\ 2M+4\cdot(N-4)+(i-N+1)\cdot M+j & \text{when } N-1 \leqslant i \leqslant N, 1 \leqslant j \leqslant M. \end{cases}$$

With the above definitions, equation system (5) can be written as the following matrix form

$$[A_{IB}]\cdot\{W_B\}+[A_{II}]\cdot\{W_I\} = \Omega^2\cdot\{W_I\}. \tag{13}$$

Similarly, eqns (6)–(10) can be put in the following matrix form

$$[A_{BB}]\cdot\{W_B\}+[A_{BI}]\cdot\{W_I\} = 0. \tag{14}$$

Substituting eqn (14) into eqn (13) gives the final eigenvalue equation system as

$$\{[A_{II}]-[A_{IB}]\cdot[A_{BB}]^{-1}\cdot[A_{BI}]\}\cdot\{W_I\} = \Omega^2\cdot\{W_I\}. \tag{15}$$

It is noted that the dimensions of matrices $[A_{II}]$, $[A_{BB}]$, $[A_{IB}]$ and $[A_{BI}]$ are $(N-4)\times(M-4)$ by $(N-4)\times(M-4)$, $(4N+4M-16)$ by $(4N+4M-16)$, $(N-4)\times(M-4)$ by $(4N+4M-16)$, and $(4N+4M-16)$ by $(N-4)\times(M-4)$, respectively. The CBCGE approach is a general method for implementing the boundary conditions. Although it is demonstrated by a plate configuration of C-SS-F-F, it can be applied to any type of boundary conditions including the combination of clamped and simply supported edge conditions. However, as will be seen in the following, it requires more virtual storage and computational effort than the SBCGE approach for the combination of clamped and simply supported edge conditions.

4. RESULTS AND DISCUSSION

The proposed CBCGE method is applied to study the free vibration of a rectangular plate with a variety of boundary conditions. The coordinates of grid points are chosen as

$$X_i = \frac{1-\cos\left(\frac{i-1}{N-1}\cdot\pi\right)}{2}, \quad i = 1,2,\ldots,N, \tag{16a}$$

$$Y_j = \frac{1-\cos\left(\frac{j-1}{M-1}\cdot\pi\right)}{2}, \quad j = 1,2,\ldots,M. \tag{16b}$$

First, the CBCGE results are compared with the SBCGE results for plates with simple boundary conditions. It was found that, for any combination of simply supported and clamped boundary conditions, both the CBCGE and the SBCGE methods provide exactly

Table 1. Comparison of run time on PC 486 DX50

Mesh size	11×11	15×15	18×18	21×21
CBCGE (seconds)	4.54	20.80	67.01	161.56
SBCGE (seconds)	1.60	9.75	37.93	101.97

the same numerical results. However, the CBCGE method requires more virtual storage and computational effort. As shown above, the CBCGE method needs to store four matrices $[A_{II}]$, $[A_{BB}]$, $[A_{IB}]$, $[A_{BI}]$, while the SBCGE method needs to store only one matrix $[A_{II}]$. As the number of grid points increases by a small number, the dimensions of matrices $[A_{BB}]$, $[A_{IB}]$, $[A_{BI}]$, will increase considerably. For example, when the mesh size is taken as 11×11, the dimensions of matrices $[A_{BB}]$, $[A_{IB}]$, $[A_{BI}]$, are 72×72, 49×72, 72×49, respectively, and when the mesh size is changed to 15×15, the dimensions of the above three matrices are changed to 104×104, 121×104, 104×121, accordingly. Except for virtual storage, the CBCGE method also requires more operations for the inversion of the matrix $[A_{BB}]$ and other computations. Table 1 shows the run time on an IBM compatible PC 486 DX50 required by the CBCGE and SBCGE methods for the solution of a SS-SS-SS-SS square plate. It was found that, when the mesh size is kept the same, the computer run time required by each of the approaches is nearly the same for different sets of boundary conditions. It can be observed from Table 1 that the SBCGE method requires much less computing time than the CBCGE method, especially for the case of a coarse mesh. Thus, we can conclude that, for simply supported and clamped edge conditions, the SBCGE method is more efficient than the CBCGE method. The advantage of the CBCGE method is its generality, which can be applied to any combination of simply supported, clamped, and free edge conditions.

Table 2 shows the natural frequencies of the first five modes for a square plate. The CBCGE results of six plate configurations, namely, SS-SS-SS-F, SS-C-SS-F, SS-F-SS-F, C-C-C-F, C-F-C-F, C-F-SS-F, are tabulated together with the data from Leissa (1973) in parentheses. The mesh size used for the CBCGE results is 15×15. It should be indicated that Leissa's results for the SS-SS-SS-F, SS-C-SS-F, and SS-F-SS-F plates are exact, and that the remaining three sets of results are from the Rayleigh–Ritz method with beam functions for the displacements, taking nine terms, i.e., three beam functions in each

Table 2. Natural frequencies of a square plate without free corner

Plate type	Ω_1	Ω_2	Ω_3	Ω_4	Ω_5
SS-SS-SS-F	11.685	27.756	41.197	59.066	61.861
	(11.685)	(27.756)	(41.197)	(59.066)	(61.861)
	0.000%	0.000%	0.000%	0.000%	0.000%
SS-C-SS-F	12.687	33.065	41.702	63.016	72.400
	(12.687)	(33.065)	(41.702)	(63.015)	(72.398)
	0.000%	0.000%	0.000%	0.002%	0.003%
SS-F-SS-F	9.631	16.135	36.726	38.945	46.739
	(9.631)	(16.135)	(36.726)	(38.945)	(46.738)
	0.00%	0.000%	0.000%	0.000%	0.002%
C-C-C-F	24.025	40.147	63.494	76.845	80.901
	(24.020)	(40.039)	(63.493)	(76.761)	(80.713)
	0.021%	0.270%	0.002%	0.109%	0.233%
C-F-C-F	22.237	26.594	43.871	61.407	67.659
	(22.272)	(26.529)	(43.664)	(61.466)	(67.549)
	−0.157%	0.245%	0.474%	−0.096%	0.163%
C-F-SS-F	15.232	20.693	39.882	49.500	56.393
	(15.285)	(20.673)	(39.775)	(49.730)	(56.617)
	−0.347%	0.097%	0.269%	−0.462%	−0.396%

The values in parentheses are the frequency data of Leissa (1973). Percentage values indicate relative difference with respect to Liessa'a data.

Table 3. Natural frequencies of a square plate with free corners

Plate type	Ω_1	Ω_2	Ω_3	Ω_4	Ω_5
SS-SS-F-F	2.549	17.316	17.662	36.576	51.039
	(3.369)	(17.407)	(19.367)	(38.291)	(51.324)
	−24.34%	−0.523%	−8.804%	−4.479%	−0.555%
C-C-F-F	7.873	23.615	23.873	44.587	62.730
	(6.942)	(24.034)	(26.681)	(47.785)	(63.039)
	13.411%	−1.743%	−10.524%	−6.692%	−0.872%
C-SS-F-F	5.780	20.703	20.926	40.296	52.255
	(5.364)	(19.171)	(24.768)	(43.191)	(53.000)
	7.755%	7.991%	−15.512%	−6.703%	−1.406%
SS-F-F-F	5.161	14.725	23.082	24.156	46.296
	(6.648)	(15.023)	(25.492)	(26.126)	(48.711)
	−22.368%	−1.984%	−16.042%	−7.540%	−4.958%
C-F-F-F	3.898	9.459	20.206	26.150	26.500
	(3.492)	(8.525)	(21.429)	(27.331)	(31.111)
	11.627%	10.956%	−5.707%	−4.321%	−14.821%
F-F-F-F	10.303	19.596	22.146	30.026	30.803
	(13.489)	(19.789)	(24.432)	(35.024)	(35.024)
	−23.619%	−0.975%	−9.357%	−14.270%	−12.052%

The values in parentheses are the frequency data of Leissa (1973). Percentage values indicate relative difference with respect to Leissa's data.

direction, for each symmetry class. The remaining frequencies for the approximate solutions are all upper bounds on the exact values. It is noted that every plate configuration in Table 2 consists of at least one free edge, and does not include any free corner. The percentage values represent the relative difference of the CBCGE results with respect to Leissa's data. They are defined as

$$\text{relative difference } \% = 100 \times (\text{CBCGE result} - \text{Leissa's data})/\text{Leissa's data}.$$

It can be observed from Table 2 that all the CBCGE results agree with the data from Leissa (1973) to within 1%. It was found that, if one pair of opposite edges are simply supported, the CBCGE results can match Leissa's data up to three decimal digits. The numerical results of C-C-C-F, C-F-C-F, C-F-SS-F cases are less accurate than the results of SS-SS-SS-F, SS-C-SS-F, and SS-F-SS-F cases.

For the case of plate configurations with at least one free corner, it was found that the numerical results are very sensitive to the grid point distribution. When the grid point distribution is taken from eqn (16), the numerical results are quite in error. This can be seen in Table 3, where the computed natural frequencies of the first five modes for a square plate with at least one free corner are listed together with the data from Leissa (1973) in parentheses. The numerical results are obtained using a mesh size of 15×15, and the coordinates of the grid points are taken from eqn (16). All six possible plate configurations with free corners, namely, SS-SS-F-F, C-C-F-F, C-SS-F-F, SS-F-F-F, C-F-F-F, F-F-F-F, are considered in Table 3. The percentage values were defined earlier. It can be seen that the numerical results for these cases do not exhibit any convergence trend. To improve the accuracy of the numerical results, the following grid point distribution was used

$$X = 3 \cdot \xi^2 - 2 \cdot \xi^3 \tag{17a}$$

$$Y = 3 \cdot \eta^2 - 2 \cdot \eta^3 \tag{17b}$$

where

Table 4. Convergence of SS-SS-F-F and C-C-F-F results

	Ω_1	Ω_2	Ω_3	Ω_4	Ω_5
			SS-SS-F-F		
Leissa (1973)	3.369	17.407	19.367	38.291	51.324
$N = M = 6$	3.257	21.439	22.277	47.072	47.072
	−3.324%	23.163%	15.026%	22.867%	−8.285%
$N = M = 8$	3.316	17.375	19.282	38.538	49.448
	−1.573%	−0.184%	−0.439%	0.645%	−7.655%
$N = M = 10$	3.349	17.319	19.238	38.130	51.074
	−0.594%	−0.506%	−0.666%	−0.420%	−0.487%
$N = M = 12$	3.363	17.317	19.293	38.218	51.032
	−0.178%	−0.517%	−0.382%	−0.191%	−0.569%
			C-C-F-F		
Leissa (1973)	6.942	24.034	26.681	47.785	63.039
$N = M = 6$	1.826	37.001	37.001	70.880	70.880
	−73.696%	53.953%	38.679%	48.331%	12.438%
$N = M = 8$	5.254	26.340	36.612	44.769	45.363
	−24.316%	9.595%	37.221%	−6.312%	−28.040%
$N = M = 10$	7.145	24.588	26.564	47.480	61.938
	2.924%	2.305%	−0.439%	−0.638%	−1.747%
$N = M = 12$	6.982	24.193	26.683	47.909	62.489
	0.576%	0.662%	0.007%	0.259%	−0.872%

Percentage values indicate relative difference with respect to the data of Leissa (1973).

$$\xi_i = \frac{1-\cos\left(\frac{i-1}{N-1}\cdot\pi\right)}{2}, i = 1,2,\ldots,N,$$

$$\eta_j = \frac{1-\cos\left(\frac{j-1}{M-1}\cdot\pi\right)}{2}, j = 1,2,\ldots,M.$$

It is noted that eqn (17) is based on eqn (16) with grid points further stretched near the boundary. When the coordinates of the grid points are computed from eqn (17), the numerical results are greatly improved. This can be observed from Tables 4–6, where a square plate is considered. Table 4 shows the convergence of SS-SS-F-F and C-C-F-F results. The convergence of C-SS-F-F and SS-F-F-F results is given in Table 5, and the convergence of C-F-F-F and F-F-F-F results is displayed in Table 6. The convergence trends of the numerical results for the above-mentioned six cases are obvious. Again, the percentage values in these tables represent the relative difference with respect to the data of Leissa (1973). When the mesh size is taken as 6×6, the numerical results are quite erratic, especially for the case of F-F-F-F, where all computed frequencies are zero. When the mesh size is refined to 10×10, the accuracy of the numerical results is greatly improved, especially for the cases of SS-SS-F-F, SS-F-F-F, where the relative differences of the numerical results with respect to Leissa's data are well below 1% for the first five natural frequencies. When the mesh size is further refined to 12×12, the relative differences of all six cases are well below 1%. This demonstrates that the proposed new grid point distribution is more suitable for plate configurations with free edges and corners. For the better comparison of present results with available data in the case of completely free plates, the work of Leissa and Narita (1984) is also included in Table 6. Like the work of Leissa (1973), Leissa and Narita (1984) also used Rayleigh–Ritz method to obtain the upper bounds of natural frequencies.

Table 5. Convergence of C-SS-F-F and SS-F-F-F results

	Ω_1	Ω_2	Ω_3	Ω_4	Ω_5
			C-SS-F-F		
Leissa (1973)	5.364	19.171	24.768	43.191	53.000
$N = M = 6$	2.237	21.768	37.262	37.262	37.262
	−58.296%	13.547%	50.444%	−13.727%	−29.694%
$N = M = 8$	4.812	20.097	39.680	39.680	39.715
	−10.291%	4.830%	60.207%	−8.129%	−25.066%
$N = M = 10$	5.416	19.954	24.446	42.982	52.892
	0.969%	4.084%	−1.300%	−0.484%	−0.204%
$N = M = 12$	5.402	19.219	25.005	43.372	52.702
	0.708%	0.250%	0.957%	0.419%	−0.562%
			SS-F-F-F		
Leissa (1973)	6.648	15.023	25.492	26.126	48.711
$N = M = 6$	6.642	18.202	18.202	18.202	18.202
	−0.090%	21.161%	−28.597%	−30.330%	−62.633%
$N = M = 8$	6.542	14.927	25.445	25.965	47.270
	−1.594%	−0.639%	−0.184%	−0.616%	−2.958%
$N = M = 10$	6.597	14.900	25.247	25.971	48.445
	−0.767%	−0.819%	−0.961%	−0.593%	−0.546%
$N = M = 12$	6.636	14.901	25.388	26.003	48.469
	−0.181%	−0.812%	−0.408%	−0.471%	−0.497%

Percentage values indicate relative difference with respect to the data of Leissa (1973).

Table 6. Convergence of C-F-F-F and F-F-F-F results

	Ω_1	Ω_2	Ω_3	Ω_4	Ω_5
			C-F-F-F		
Leissa (1973)	3.492	8.525	21.429	27.331	31.111
$N = M = 6$	1.362	2.527	35.741	35.741	35.741
	−60.997%	−70.358%	66.788%	30.771%	14.882%
$N = M = 8$	0.598	4.882	25.193	28.160	31.337
	−82.875%	−42.733%	17.565%	3.033%	0.726%
$N = M = 10$	3.298	9.512	21.335	28.156	30.838
	−5.556%	11.578%	−0.439%	3.019%	−0.878%
$N = M = 12$	3.485	8.604	21.586	27.230	31.358
	−0.200%	0.927%	0.747%	−0.370%	0.794%
			F-F-F-F		
Leissa (1973)	13.489	19.789	24.432	35.024	35.024
Leissa & Narita (1984)	13.468	19.596	24.271	34.801	34.801
$N = M = 6$	0	0	0	0	0
$N = M = 8$	13.161	19.558	24.131	35.028	35.043
	−2.432%	−1.167%	−1.232%	0.011%	0.054%
$N = M = 10$	13.281	19.605	24.258	34.627	34.642
	−1.542%	−0.930%	−0.712%	−1.133%	−1.091%
$N = M = 12$	13.454	19.597	24.271	34.815	34.817
	−0.259%	−0.970%	−0.659%	−0.597%	−0.591%

Percentage values indicate relative difference with respect to the data of Leissa (1973).

However, they used 16 instead of 9 terms for each symmetry class. Thus, the results of Leissa and Narita (1984) are more accurate than those of Leissa (1973). It can be seen from Table 6 that the present results are closer to the data of Leissa and Narita (1984) than the results of Leissa (1973). This indicates that the present results are very accurate.

5. CONCLUSIONS

In this paper, a new approach is proposed for implementing the general boundary conditions in the GDQ free vibration analysis of rectangular plates. The present approach directly couples the discretized boundary conditions with the discretized governing equations. It may be applied to any general boundary condition. For the case of simply supported and clamped boundary conditions, both the CBCGE and the SBCGE methods provide exactly the same numerical results. However, the SBCGE method is more attractive for this case since it requires much less virtual storage and computational effort. The CBCGE method is suitable for any general type of boundary condition, whereas the SBCGE method is not applicable to free edges. For a plate configuration without a free corner, the grid point distribution based on the cosine function works well and the corresponding numerical results are very accurate. However, for plate configurations with at least one free corner, the numerical results based on the grid point distribution of cosine function are quite erratic. To improve the accuracy, a new grid point distribution is suggested. Numerical experiments show that the proposed grid point distribution works very well for all the possible plate configurations with free corners. When the mesh size is taken as 12×12, the relative difference of numerical results with respect to Leissa's data is well below 1% for the first five natural frequencies. This demonstrates that the proposed new grid point distribution is more suitable for plates with free edges and free corners.

REFERENCES

Bert, C. W., Wang, X. and Striz, A. G. (1993) Differential quadrature for static and free vibration analysis of anisotropic plates. *International Journal of Solids and Structures* **30,** 1737–1744.

Jang, S. K., Bert, C. W. and Striz, A. G. (1989) Application of differential quadrature to static analysis of structural components. *International Journal of Numerical Methods in Engineering* **28,** 561–577.

Leissa, A. W. (1973) The free vibration of rectangular plates. *Journal of Sound and Vibration* **31,** 257–293.

Leissa, A. W. and Narita, Y. (1984) Vibrations of completely free shallow shells of rectangular planform. *Journal of Sound and Vibration* **96,** 207–218.

Shu, C. and Du, H. (1996) Implementation of clamped and simply supported boundary conditions in the GDQ free vibration analysis of beams and plates. *International Journal of Solids and Structures* **34,** 819–835.

Wang, X. and Bert, C. W. (1993) A new approach in applying differential quadrature to static and free vibrational analyses of beams and plates. *Journal of Sound and Vibration* **162,** 566–572.